

# Effects of disorder on the non-zero temperature Mott Transition

M. C. O. Aguiar,<sup>1</sup> V. Dobrosavljević,<sup>2</sup> E. Abrahams,<sup>1</sup> and G. Kotliar<sup>1</sup>

<sup>1</sup>*Center for Materials Theory, Serin Physics Laboratory,*

*Rutgers University, 136 Frelinghuysen Road, Piscataway, New Jersey 08854*

<sup>2</sup>*Department of Physics and National High Magnetic Field Laboratory, Florida State University, Tallahassee, FL 32306*

The physics of the metal-insulator coexistence region near the non-zero temperature Mott transition is investigated in presence of weak disorder. We demonstrate that disorder reduces the temperature extent and the general size of the coexistence region, consistent with recent experiments on several Mott systems. We also discuss the qualitative scenario for the disorder-modified Mott transition, and present simple scaling arguments that reveal the similarities to, and the differences from, the clean limit.

PACS numbers: 71.10.Fd, 71.30.+h, 71.55.Jv

## I. INTRODUCTION AND MOTIVATION

The physics of the metal-insulator transition has continued to attract considerable interest in recent years. Substantial progress has been achieved in understanding the behavior near the interaction-driven transition, where Dynamical Mean Field Theory<sup>1</sup> (DMFT) has been very successful in explaining the behavior of several classes of materials ranging from transition metal oxides such as  $V_2O_3$  to organic Mott systems. This approach has been especially useful in describing the non-zero temperature behavior in the paramagnetic coexistence region between the metal and the insulator. In this regime, the two phases compete, and the resulting behavior emerges as a compromise between the energy gain to form coherent quasiparticles, and the larger entropy inherent to the incoherent insulating solution. There is not actual two-phase coexistence (as in conventional first order thermodynamic phase transitions) in this region. Rather, it is a region of parameters in which two local minima of the free energy coexist.

So far, most theoretical work has concentrated on clean systems, although several experimental studies indicate that effects of disorder are particularly important precisely in this coexistence regime. Measurements performed in compounds such as NiSSe mixtures<sup>2,3,4</sup> and  $\kappa$ -organics<sup>5,6</sup> indicate that the presence of disorder pushes down the critical temperature end point of the metal and insulator coexistence region. In particular, experiments performed on a  $NiS_2$  compound, which has much weaker disorder, show that the Mott transition occurs at 150K,<sup>2</sup> with an external applied pressure of 3 GPa, while in the substituted  $NiS_{2-x}Se_x$  compound it is seen only below 100K.<sup>4</sup> It is important to notice that applying an external pressure to these compounds is equivalent to substituting S by Se, which might suggest that the results above would be in conflict. A speculation was made that the reduction in the transition temperature would be due to the local randomness introduced with Se substitution.<sup>3</sup>

We address the theoretical issues from the perspective of the Hubbard model. It is not a priori obvious what should be the effect of disorder on the size and the tem-

perature range of the coexistence region. On the one hand, disorder tends to broaden the Hubbard bands and thus larger interaction is needed to open a Mott Hubbard gap. This may lead to a larger overall energy scale, which could stabilize the coexistence region. On the other hand, disorder generally leads to spatial fluctuations in all local quantities, an effect that could smear or decrease the jump at any first order phase transition, and thus reduce the coexistence energy scale. These considerations indicate that careful theoretical work is called for, which can address the interplay of interactions and disorder near the Mott metal-insulator transition.

A formalism that describes the effects of disorder within a DMFT approach was outlined some time ago,<sup>7</sup> but a very limited number of calculations were explicitly carried out within this framework. More recently, the approach was reexamined to investigate strong correlation effects on disorder screening,<sup>8</sup> and the related temperature dependence of transport in the metallic phase.<sup>9</sup> These results shed light on several puzzling phenomena observed in experiments on two dimensional electron systems, but did not provide a description of the physics relevant to the coexistence region at non-zero temperature.

In this paper we examine the phase diagram for the Mott transition in the presence of moderate disorder at non-zero temperature within the DMFT approach.<sup>7</sup> We present results describing the evolution of the coexistence region, showing that disorder generally reduces its size, in agreement with experiments. Our results give a physical picture that describes the gradual destruction of quasiparticles as the Mott insulator is approached, and establish the qualitative modification of the critical behavior resulting from the presence of disorder.

Our findings are valid in the regime of strong correlations but weak to moderate disorder, where Anderson localization effects, which are neglected in our theory, can be safely ignored. The latter have been included in earlier zero temperature DMFT-based strong correlation calculations.<sup>10,11</sup> In particular, we mention that our lowest temperature results are consistent with the  $T = 0$  result at weak disorder of Byczuk et al,<sup>11</sup> but give the temperature dependence of the metal-insulator coexistence region.

## II. NON-ZERO TEMPERATURE DMFT FOR DISORDERED ELECTRONS

We consider a half-filled Hubbard model in the presence of random site energies, as given by the hamiltonian

$$H = -t \sum_{\langle ij \rangle \sigma} c_{i\sigma}^\dagger c_{j\sigma} + \sum_{i\sigma} \varepsilon_i n_{i\sigma} + U \sum_i n_{i\uparrow} n_{i\downarrow}. \quad (1)$$

Here  $c_{i\sigma}^\dagger$  ( $c_{i\sigma}$ ) creates (destroys) a conduction electron with spin  $\sigma$  on site  $i$ ,  $n_{i\sigma} = c_{i\sigma}^\dagger c_{i\sigma}$  is the particle number operator,  $t$  is the hopping amplitude, and  $U$  is the on-site repulsion. The random site energies  $\varepsilon_i$  are assumed to have a uniform distribution of width  $W$ .

Within DMFT for disordered electrons,<sup>7</sup> a quasiparticle is characterized by a local but site-dependent<sup>12</sup> self-energy function  $\Sigma_i(\omega) = \Sigma(\omega, \varepsilon_i)$ . To calculate these self-energies, the problem is mapped onto an *ensemble* of Anderson impurity problems<sup>7</sup> embedded in a self-consistently calculated conduction bath. In this approach, only quantitative details of the solution depend on the details of the electronic band structure; in the following we concentrate on a semi-circular model density of states. In this particular case, the hybridization function is given by

$$\Delta(\omega) = t^2 \bar{G}(\omega) \quad (2)$$

and the average local Green's function,  $\bar{G}(\omega)$ , is obtained by imposing the following self-consistent condition

$$\bar{G}(\omega) = \left\langle \frac{1}{\omega - \varepsilon_i - \Delta(\omega) - \Sigma_i(\omega)} \right\rangle, \quad (3)$$

where  $\langle \dots \rangle$  indicates the arithmetic average over the distribution of  $\varepsilon_i$ .

To solve the single-impurity problems at non-zero temperature for different site energies, we mostly used the iterated perturbation theory (IPT) method of Kajuter and Kotliar.<sup>13,14</sup> However, to check the accuracy of the results, in several instances we also used the numerically exact quantum Monte Carlo method as an impurity solver, and generally found good qualitative and even quantitative agreement, supporting the validity of our IPT predictions in the relevant parameter ranges. Throughout the paper we express all energies in units of the bandwidth.

## III. PHASE DIAGRAM

We first examine the evolution of the coexistence region as disorder is introduced. Within this region, both metallic and insulating solutions are found, depending on the initial guess used in the iterative scheme for solving the self-consistency condition. Typical results are presented in Fig. 1, showing the phase diagram obtained within DMFT-IPT at non-zero temperature, for varying

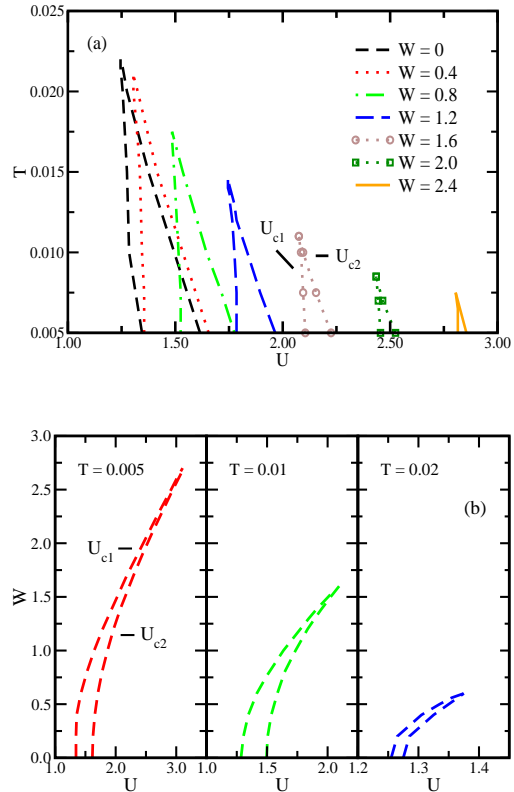


FIG. 1: Phase diagram for the disordered Hubbard model at non-zero temperature. (a)  $(U, T)$  diagram for different disorder strengths. (b)  $(U, W)$  diagram at different temperatures.  $U_{c1}$  and  $U_{c2}$  lines are indicated in one of the plots, but similar definitions apply to the other results as well.

levels of disorder  $W$ . For each level of disorder [shown in panel (a)] or temperature [shown in panel (b)], the first (from left) of the two lines, the so-called  $U_{c1}$ , indicates the stability boundary (i.e. the spinodal) of the insulating solution. Conversely, the second of the two lines, identified as  $U_{c2}$ , represents the boundary of the metallic solution. The coexistence region is found between these two lines, i.e. for  $U_{c1} < U < U_{c2}$ . Our results are in good quantitative agreement with previous results obtained in the  $T = 0$  limit in presence of disorder,<sup>8</sup> and also with non-zero temperature results in absence of disorder.<sup>1</sup> As the disorder increases, the metal-insulator transition generally moves to larger  $U$ . Physically, this reflects the fact that disorder broadens the bands and smears the gap, making it harder for the Mott-Hubbard gap to open, so that a larger  $U$  is necessary for the transition. At the same time, the temperature-dependent coexistence region is found to shrink [Fig. 1(a)], persisting only below a critical end-point temperature  $T_c(W)$ . At any given temperature, the principal effects of introducing disorder [Fig. 1(b)] are as follows: (1) both the  $U_{c1}$  and  $U_{c2}$  lines move towards larger interaction potential; (2) the

lines become closer to each other as disorder increases. In fact, they both approach the  $W = U$  line as  $W \rightarrow \infty$ .

Having obtained these results in quantitative detail, we would like to understand the physical origin of this behavior. In the following we present simple analytical arguments relating the non-zero temperature aspects of the coexistence region to the evolution of its ground state properties. Our strategy is motivated by the following observations: (a) the shape of the non-zero temperature coexistence region [Fig. 1(a)] remains *very similar* at different values of disorder; (b) its size, both in terms of temperature and in terms of  $U$ -range, shrinks as disorder increases. This suggests that the physical mechanism for the destruction of the coexistence region as the temperature increases is similar to that of the clean limit, where it is governed by decoherence processes due to inelastic electron-electron scattering. Therefore, we begin our analysis by concentrating on the clean limit, where we show how simple estimates for the critical end-point temperature  $T_c$  can be obtained.

#### IV. COEXISTENCE REGION IN THE CLEAN LIMIT

The coexistence region at non-zero temperature is delimited by the two spinodal lines  $U_{c1}(T)$  and  $U_{c2}(T)$ ; the critical end-point temperature  $T_c$  is reached when these two boundaries intersect. To estimate  $T_c$  using the  $T = 0$  properties of the model, we need to understand the temperature dependence of each of these lines.

##### A. Insulating spinodal

The insulating spinodal  $U_{c1}(T)$  essentially corresponds to the closing of the gap separating the two Hubbard bands in the Mott insulator. Its temperature dependence should thus reflect that of the Hubbard bands. In contrast to the correlated metallic state close to the Mott transition, the insulating solution is not characterized by a small energy scale in the coexistence region. Accordingly, it is not expected to have strong temperature dependence; its weak temperature dependence reflects activated processes across the Mott-Hubbard gap. Such activations only lead to (exponentially) weak rounding/broadening of the Hubbard bands, which should very slowly reduce  $U_{c1}(T)$  as temperature increases. Such behavior is indeed clearly seen in our results. This temperature dependence is, however, much weaker than that characterizing  $U_{c2}(T)$ . For purposes of roughly estimating  $T_c$ , to leading order we can ignore this weak temperature dependence, so that

$$U_{c1}(T) \approx U_{c1}(T = 0). \quad (4)$$

##### B. Metallic spinodal

In the vicinity of the Mott transition, the metallic solution is characterized by a low energy scale corresponding to the coherence temperature  $T^*$  of a low-temperature Fermi liquid.<sup>1</sup> Above  $T^*$  the heavy quasiparticles are destroyed, and the metallic solution becomes unstable. To estimate  $U_{c2}(T)$  we need to determine how this coherence temperature varies as the transition is approached. From detailed studies of the clean<sup>1</sup> and disordered<sup>9</sup> Hubbard models within DMFT, it is known that this coherence temperature can be estimated as

$$T^* \approx AT_F Z \quad (5)$$

where  $T_F$  is the Fermi temperature,  $A$  is a constant of order one, and  $Z$  is the quasiparticle (QP) weight defined as

$$Z = \left[ 1 - \frac{\partial}{\partial \omega} \text{Im} \Sigma(\omega) \Big|_{\omega \rightarrow 0} \right]^{-1}. \quad (6)$$

The behavior of  $Z$  is well known in the clean limit,<sup>1</sup> where it decreases linearly as  $U$  increases toward the metallic spinodal, viz.

$$Z = C[U_{c2}(0) - U]. \quad (7)$$

From numerical studies,<sup>1</sup> the proportionality constant  $C \approx 0.45$ . Therefore, the coherence temperature can be written as

$$T^*(U) = ACT_F[U_{c2}(0) - U]. \quad (8)$$

We can now estimate the temperature dependence of  $U_{c2}(T)$  as that value of the interaction needed to set  $T^*(U) = T$ , i.e.

$$T = ACT_F[U_{c2}(0) - U_{c2}(T)].$$

In other words

$$U_{c2}(T) \approx U_{c2}(0) - BT, \quad (9)$$

where  $B = 1/ACT_F$ . From our numerical results [see Fig. 1(a)] we find  $B \approx 22$ , giving  $A \approx 0.2$ , in reasonable agreement<sup>15</sup> with estimates<sup>9</sup> from the literature.

Using these expressions for  $U_{c1}(T)$  and  $U_{c2}(T)$ , we arrive at the estimate for the critical end-point temperature

$$T_c \approx [U_{c2}(0) - U_{c1}(0)]/B, \quad (10)$$

which agrees within 10% with our numerical results (see Fig. 7).

#### V. CRITICAL BEHAVIOR IN PRESENCE OF DISORDER

Encouraged by the success of our analytical description of the coexistence regime in the clean limit, we now

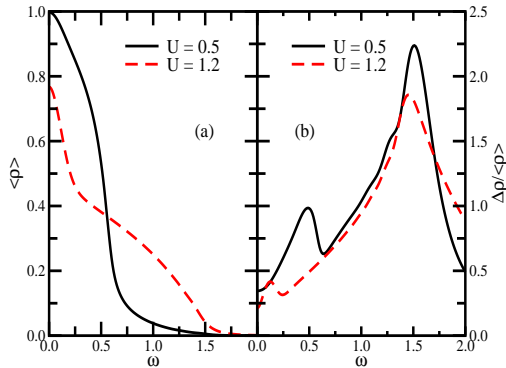


FIG. 2: (a) Average spectral function and (b) relative deviation of the distribution of  $\rho_i(\omega)$ ,  $\Delta\rho/\langle\rho\rangle$ , as a function of frequency for different values of the interaction potential.  $\Delta\rho$  is the standard deviation of the distribution of  $\rho_i(\omega)$ , which is given by  $\sqrt{\sum_i(\rho_i(\omega) - \langle\rho_i(\omega)\rangle)^2/(N-1)}$ , where  $N$  is the number of local site energies considered. Other parameters used were  $T = 0.05$  and  $W = 1.0$ .

turn our attention to the effects of disorder. As in the clean limit, we would like to relate the finite temperature properties to the critical behavior of the quasiparticles at  $T = 0$ . To do this, we therefore concentrate on describing the critical behavior in presence of disorder.

The principal new feature introduced by disorder within the DMFT scheme is the spatial variation of the spectral function,  $\rho_i(\omega)$ . This is shown in Fig. 2 at all energy scales: on the left we have the average spectral function and on the right the relative deviation of its distribution, in the metallic phase. For each value of the interaction potential, the distribution of  $\rho_i(\omega)$  presents a large dip at  $\omega \approx 0$  and becomes broader as the frequency increases. This comes from the fact that at small frequencies the system is in the Fermi liquid regime. At finite temperature we observe the reminiscence of the perfect disorder screening seen at  $T = 0$  close to the Mott transition.<sup>8</sup> For large frequencies, the quasiparticle regime is no more valid and the appropriate description is in terms of Hubbard bands, resulting in an increase of the fluctuation in  $\rho_i(\omega)$ .

In the disordered case, the self-energy function  $\Sigma_i(\omega)$  presents site-to-site fluctuations, which lead to the spatial variations of the spectral function discussed above. The QP weights  $Z_i = Z(\varepsilon_i)$  now depend on the local site energy  $\varepsilon_i$ . To properly describe the approach to the Mott transition, we therefore must follow the evolution of the entire function  $Z(\varepsilon_i)$  as the transition is approached.<sup>16</sup>

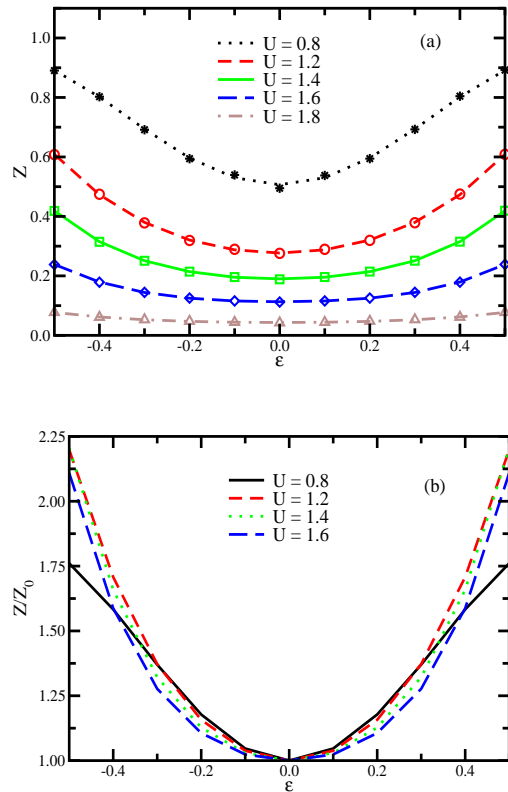


FIG. 3: (a) Quasiparticle weight as a function of the on-site energy for different values of the interaction potential as the  $U_{c2}$  line is approached, for disorder strength  $W = 1.0$ . The symbols are the numerical data, while the lines correspond to the fitting indicated in the plot, that is to a function with even exponents in  $\varepsilon$ . (b) Fitted results for  $Z$  divided by  $Z_0$  (the quasiparticle weight for  $\varepsilon = 0$ ) as a function of  $\varepsilon$ , showing that close to the MIT the curves for different  $U$  scale. These results were obtained at a low but finite temperature  $T = 0.005$ .

### A. Behavior of local QP weights

Given the self-consistent solution of our ensemble of impurity models, we calculate the local QP weights as

$$Z_i = \left[ 1 - \frac{\partial}{\partial \omega} \text{Im} \Sigma_i(\omega) \Big|_{\omega \rightarrow 0} \right]^{-1}. \quad (11)$$

Typical results are shown in Fig. 3(a), where we plot  $Z_i = Z(\varepsilon_i)$  at  $T = 0.005$ , for disorder strength  $W = 1$ , as the metallic spinodal is approached by increasing the interaction  $U$  toward  $U_{c2} \approx 1.9$ . We first observe that for small  $U$ , away from the transition, the QP weights  $Z_i$  have strong  $\varepsilon_i$  dependence, with the smallest  $Z_i$  at  $\varepsilon_i = 0$ . Physically, this reflects the tendency for correlation effects (suppression of  $Z$ ) to be the strongest on sites which are locally close to half-filling (singly occupied). Nonzero site energies favor the local occupation

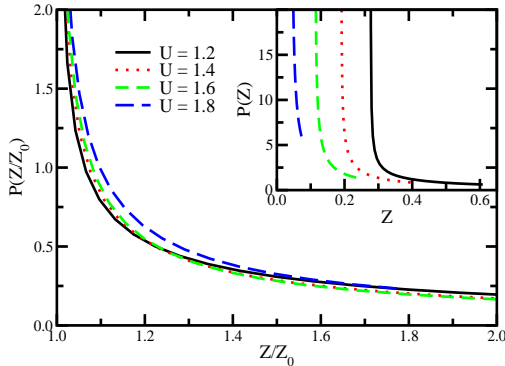


FIG. 4: Distribution of quasiparticle weight for different values of the interaction potential. The main plot shows how the curves collapse when we look at  $Z/Z_0$ . The inset shows the results for  $Z$  itself. Other parameters as in Fig. 3.

departing from half-filling, thus reducing the correlation effect, and increasing  $Z_i$ .

As  $U$  increases, all the  $Z_i$ 's decrease, as in the clean case. But how does this affect the distribution of QP weights  $Z_i = Z(\varepsilon_i)$ ? At first glance it seems that the  $\varepsilon_i$  dependence becomes weaker, but a closer look reveals this not to be the case. As we shall now demonstrate, all the  $Z_i$ 's decrease linearly near the transition, i.e. they assume the form

$$Z(U, \varepsilon_i) = K(\varepsilon_i)[U_{c2} - U], \quad (12)$$

where only the prefactor  $K(\varepsilon_i)$  depends on  $\varepsilon_i$ . If, to leading order, these prefactors remain independent of the distance to the spinodal, then the entire family of curves  $Z(U, \varepsilon_i)$  can all be collapsed on a single scaling function. To verify this hypothesis, we define reduced QP weights

$$Z^*(\varepsilon_i) = Z(U, \varepsilon_i)/Z(U, 0). \quad (13)$$

If our scaling ansatz is valid, then the  $Z^*(\varepsilon_i)$  should approach a non-zero limit as  $U \rightarrow U_{c2}$ , i.e. they should all collapse onto a single scaling function. As shown in Fig. 3(b), this behavior is observed only for  $U$  sufficiently close to  $U_{c2}$  [note that the data for  $U = 0.8$  (further from the transition) show deviations from leading scaling]. This is precisely what we expect, since such simple scaling behavior typically occurs only within a critical region close to the metallic spinodal.

### B. Distribution $P(Z_i)$ of local QP weights

Equivalently, we can characterize the QP weights by their probability distribution function  $P(Z_i)$ . Typical results for  $P(Z_i)$  are shown in the inset of Fig. 4. As the  $Z_i$  decrease near the transition, the distribution function  $P(Z_i)$  changes its form and narrows down. However, if

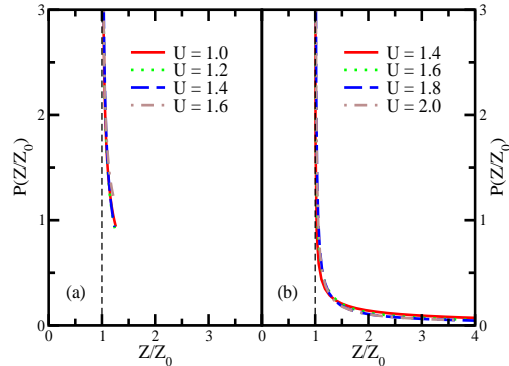


FIG. 5: Distribution of  $Z/Z_0$  for (a) smaller ( $W = 0.5$ ) and (b) larger ( $W = 1.5$ ) disorder than the one in Fig. 4. Other parameters used was  $T = 0.005$ .

our scaling hypothesis is valid, then the *shape* of this distribution should approach a “fixed-point” form very close to the transition. More precisely, we expect the distribution for reduced QP weights  $P(Z_i^*)$  to collapse to a single scaling function close to  $U_{c2}$ . Results confirming precisely such behavior are presented in Fig. 4.

An interesting question relates to the precise form of the fixed-point distribution function  $P(Z_i^*)$ , and how it may depend on disorder. In the clean limit, obviously, it reduces to  $\delta(Z_i^* - 1)$  indicating that spatial fluctuations are suppressed. As the disorder increases,  $P(Z_i^*)$  becomes very broad (as shown in Fig. 5), reflecting large site-to-site fluctuations in the local QP weights. This behavior may be regarded as a precursor of electronic Griffiths phases,<sup>17</sup> which emerge for stronger disorder, as found within *statDMFT* approaches.<sup>10</sup>

In essential contrast to the clean limit, the approach to the Mott transition in presence of disorder thus needs to be characterized by the entire *probability distribution function* of QP parameters. At first glance, this may appear to require a description considerably more complex than in the absence of disorder. However, we have demonstrated that in the critical region the distributions approach a fixed point form, allowing for “single parameter scaling,” in close analogy to the clean Mott transition. This finding immediately suggests that our arguments describing the finite temperature coexistence behavior in the clean limit may successfully be extended to the disordered case as well, allowing for a complete qualitative description, which we discuss in the following section.

## VI. COEXISTENCE REGION IN PRESENCE OF DISORDER

Within the DMFT formulation, the disorder is not expected to qualitatively affect the temperature dependence of the insulating spinodal, since the forms of the

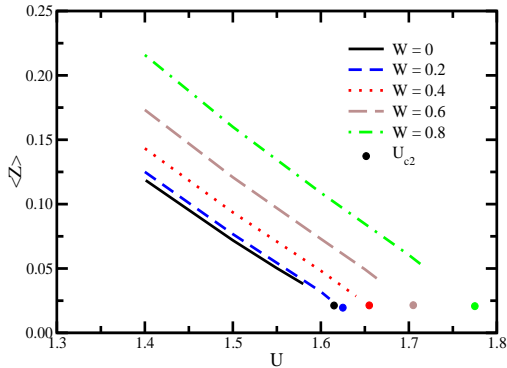


FIG. 6: Average quasiparticle weight as a function of the interaction potential for different values of disorder.

Hubbard bands remain qualitatively similar to that in the clean limit. The principal effect of disorder in the Mott insulating phase is to simply broaden the Hubbard bands, which retain well defined (sharp) band edges due to the CPA-like treatment of randomness in the DMFT limit. Indeed, our quantitative results [see Fig. 1(a)] confirm that  $U_{c1}(T) \approx U_{c1}(0)$  retains very weak temperature dependence, as in the clean case. The only modification is that  $U_{c1}(0)$  rapidly grows as disorder is increase, reflecting the disorder-induced broadening of the Hubbard bands.

The metallic solution is again found to be unstable above a certain coherence temperature  $T^*(W, U)$ , which defines the locus of the metallic spinodal  $U_{c2}(T)$ . An added subtlety is that different sites start to decohere at different temperatures, an effect that earlier work<sup>9</sup> found responsible for a nearly-linear temperature dependence of the resistivity in the disordered metallic phase. Nevertheless, sufficiently close to the Mott transition (within the coexistence region), a sharply defined temperature scale  $T^*(W, U)$  emerges where the metallic solution suddenly disappears and where the qualitative form of the spectrum changes on *all* sites. This temperature scale defines the locus of the metallic spinodal, corresponding to the equation

$$T = T^*(W, U_{c2}). \quad (14)$$

At first glance, it is anything but obvious how  $T^*(W, U)$  should be estimated. As in the clean case, the reduction of this temperature scale as the transition is approached must reflect the behavior of the local quasiparticle weights  $Z_i$ , and presumably depend on the precise form of the distribution function  $P(Z_i)$ . As we have seen, however, all the local QP weight scale in a similar fashion in the critical regime, which suggests that a reasonable estimate may be obtained simply from their

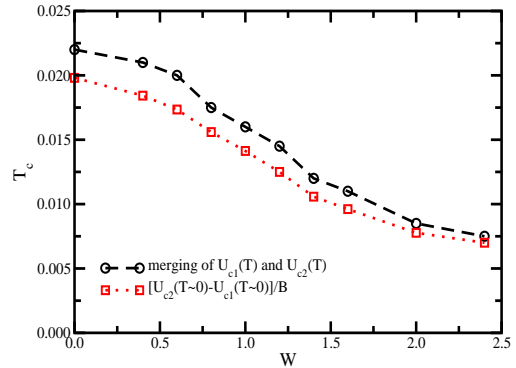


FIG. 7: Temperature at which the  $U_{c1}$  and  $U_{c2}$  lines merge in the  $(U, T)$  phase diagram as a function of disorder. The plot shows both the results obtained directly from the numerical data as well as those calculated from the linear fitting to the  $U_{c2}(T)$  line. In the latter,  $T_c$  was calculated using the values of  $U_{c1}$  at  $T = 0.005$ , except for  $W = 0$  where the result at  $T = 0.0075$  was used.

average value

$$\langle Z_i \rangle = \int d\varepsilon_i P(\varepsilon_i) Z_i. \quad (15)$$

At least for sufficiently weak disorder, we may expect that [cf. Eq. (5)]

$$T^*(W, U) \approx AT_F \langle Z_i \rangle, \quad (16)$$

where  $A \approx 0.2$  as in the clean case. Using the fact that all  $Z_i$ 's decrease linearly near the transition, we expect

$$\langle Z_i \rangle = C(W)[U_{c2}(0) - U]. \quad (17)$$

To confirm this, we explicitly calculated  $\langle Z_i \rangle$  as a function of  $U$  for different levels of disorder; the results are shown in Fig. 6. We conclude that  $C(W) \approx C(0) \approx 0.45$ . These results suggest that the metallic spinodal should take the form,

$$U_{c2}(W, T) \approx U_{c2}(W, 0) - B(W)T, \quad (18)$$

where  $B(W) \approx B(0) = 22$ . Our non-zero temperature results for  $U_{c2}(W, T)$  [see Fig. 1(a)] fully confirm these expectations. Based on these results, we finally obtain the desired expression for  $T_c(W)$  of the form

$$T_c(W) \approx [U_{c2}(W, 0) - U_{c1}(W, 0)]/B(0). \quad (19)$$

To test the proposed procedure, we have used the values for  $U_{c1}(W)$  and  $U_{c2}(W)$  at the lowest temperature of our calculation ( $T = 0.005$ ) to estimate  $T_c(W)$ . As we can see from Fig. 7, our analytical estimates are found to be in excellent agreement with results of explicit non-zero temperature calculations. The decrease of  $T_c(W)$  with disorder thus directly reflects the “shrinking” of the coexistence region at low temperature, which in its turn reflects the decrease of the energy difference between the metallic and the insulating solution.

## VII. CONCLUSIONS

In this paper we have used a DMFT approach to examine the effects of disorder on the critical behavior near the Mott metal-insulator transition, with special emphasis on non-zero temperature properties associated with the two spinodal lines  $U_{c1}$  and  $U_{c2}$ . By using a combination of numerical results and analytical arguments we have demonstrated that simple scaling behavior emerges, providing a complete description of the critical regime.

In contrast to the clean case, the presence of disorder requires one to examine the entire distribution of local spectral functions,  $\rho_i(\omega)$ , describing how the local spectra varies with position in the sample. This can be probed with scanning tunneling microscopy (STM). Notice that the distribution function describing the site dependence of  $\rho_i(\omega)$  will depend on the frequency of observation: it will be broader at higher energies [as seen in Fig. 2(b)], where a real space picture is appropriate to describe the Hubbard bands, and narrower at low frequencies, where a quasiparticle description in k space is appropriate. This is a manifestation of frequency dependence of the disorder screening discussed in an earlier paper by some of us.<sup>8</sup>

In the metallic regime, at low temperatures, the spectral function can be parametrized in terms of the distribution of quasiparticle parameters, which displays sim-

ple scaling properties. This allowed us to characterize the behavior near  $U_{c2}$  using a single parameter scaling procedure. The approach to  $U_{c2}$  thus retains a character qualitatively independent of the level of disorder, where the vanishing of quasiparticle weight signals the transmutation of itinerant electrons into localized magnetic moments.

Within the examined DMFT formulation, the region between the two spinodal lines  $U_{c1}$  and  $U_{c2}$  although reduced in size and extent cannot be completely eliminated no matter how large the disorder. Of course, these predictions are applicable only for weak enough disorder where Anderson localization effects can be ignored. Extensions of DMFT that incorporate Anderson localization mechanisms at zero temperature are available,<sup>10,11</sup> but applying these approaches to examine the non-zero temperature behavior near Mott-Anderson transitions remains an interesting research direction. The behavior at the first order transition line and the actual nucleation of either the metallic or insulating phase, between  $U_{c1}$  and  $U_{c2}$ , are also strongly modified by disorder, and this as well is left for future study.

The authors thank A. Georges and D. Tanasković for useful discussions. This work was supported by NSF grants DMR-9974311 and DMR-0234215 (VD) and DMR-0096462 (GK).

- 
- <sup>1</sup> A. Georges, G. Kotliar, W. Krauth and M.J. Rozenberg, *Rev. Mod. Phys.* **68**, 13 (1999).
- <sup>2</sup> Y. Sekine, H. Takahashi, N. Mōri, T. Matsumoto and T. Kosaka, *Physica B* **237-238**, 148 (1997).
- <sup>3</sup> M. Matsuura, H. Hiraka, K. Yamada and Y. Endoh, *Journal of Phys. Soc. of Japan* **69**, 1503 (2000).
- <sup>4</sup> S. Miyasaka, H. Takagi, Y. Sekine, H. Takahashi, N. Mōri and R.J. Cava, *Journal of Phys. Soc. of Japan* **69**, 3166 (2000).
- <sup>5</sup> P. Limelette, P. Wzietek, S. Florens, A. Georges, T.A. Costi, C. Pasquier, D. Jérôme, C. Mézière and P. Batail, *Phys. Rev. Lett.* **91**, 016401 (2003).
- <sup>6</sup> Ch. Strack, C. Akinci, B. Wolf, M. Lang, J.A. Schlueter, J. Wosnitza, D. Schweitzer and J. Müller, *cond-mat/0407478*.
- <sup>7</sup> V. Dobrosavljević and G. Kotliar, *Phys. Rev. Lett.* **71**, 3218 (1993); *Phys. Rev. B* **50**, 1430 (1994); M. Ulmke, V. Janiš and D. Vollhardt, *Phys. Rev. B* **51**, 10411 (1995).
- <sup>8</sup> D. Tanasković, V. Dobrosavljević, E. Abrahams and G. Kotliar, *Phys. Rev. Lett.* **91**, 066603 (2003).
- <sup>9</sup> M. C. O. Aguiar, E. Miranda, V. Dobrosavljević, E. Abrahams, and G. Kotliar, *Europhys. Lett.*, **67** (2), 226 (2004).
- <sup>10</sup> V. Dobrosavljević and G. Kotliar, *Phys. Rev. Lett.* **78**, 3943 (1997).
- <sup>11</sup> K. Byczuk, W. Hofstetter and D. Vollhardt, *cond-mat/0403765*.
- <sup>12</sup> The fact that the quasiparticle parameters are site-dependent was emphasized by: G. T. Zimanyi and E. Abrahams, *Phys. Rev. Lett.* **64**, 2719 (1990).
- <sup>13</sup> H. Kajueter and G. Kotliar, *Phys. Rev. Lett.* **77**, 131 (1996).
- <sup>14</sup> M. Potthoff, T. Wegner and W. Nolting, *Phys. Rev. B* **55**, 16132 (1997).
- <sup>15</sup> The definition of the coherence temperature  $T^*$  used in Ref. [9] was based on the temperature dependence of the resistivity. It was defined as the temperature where deviations from the low temperature  $T^2$  form became appreciable, and as such represents a crossover scale. That work found  $A \approx 0.1$ , which is in reasonable agreement with our present result  $A \approx 0.2$ , given the ambiguity in precisely defining the resistivity crossover scale.
- <sup>16</sup> In addition to the quasiparticle weight, the low energy excitations are also characterized by renormalized site energies describing the renormalized disorder potential. However, as discussed in Ref. [8], within the DMFT scheme the renormalized disorder is strongly screened, so the local quasiparticle weights  $Z(\varepsilon_i)$  are sufficient to characterize the critical behavior.
- <sup>17</sup> E. Miranda and V. Dobrosavljević, *Phys. Rev. Lett.* **86**, 264 (2001); D. Tanasković, E. Miranda, and V. Dobrosavljević, *Phys. Rev. B* **70**, 205108 (2004).